IN-PLANE SILICON-ON-INSULATOR OPTICAL MEMS ACCELEROMETER USING WAVEGUIDE FABRY-PEROT MICROCAVITY WITH SILICON/AIR BRAGG MIRRORS

Kazem Zandi[1], Brian Wong[2], Jing Zou[2], Roman V. Kruzelecky[2], Wes Jamroz[2] and Yves-Alain Peter[1]
[1]Ecole Polytechnique de Montréal, Montréal, Canada
[2]MPB Communications Inc., Montréal, Canada

ABSTRACT

A novel in-plane Silicon-On-insulator (SOI) optical accelerometer using a Fabry-Perot microcavity with two distributed Bragg reflectors (DBR) is presented, in which one DBR mirror is attached to two suspended proof masses. As a consequence of acceleration, the relative displacement of the movable mirror with respect to the fixed one changes the cavity length and modifies the Fabry-Perot resonance. All of the device components are fabricated by using one single fabrication step. The sensor performance could reach μg resolution with a demonstrated 2.5 nm/g sensitivity and 400 μg resolution.

INTRODUCTION

Microphotonics is a technology taking advantage of wafer-level integration of photonic components which are used as light sensors, sources, and transmitters and other forms of energy [1]. The main difficulty that microphotonics should solve is system integration. Integrating different optical components on a single substrate would contribute reducing the amount of external fiber optic interconnections, consequently decreasing the overall system mass and size, and contributing to optimize the system reliability as well as its cost efficiency.

A Fabry-Perot filter enables a highly sensitive optical detection of displacement at a sub-nanometer scale. MEMS tunable silicon Fabry-Perot (FP) filters with DBR mirrors were recently demonstrated [2-4]. These tunable filters can be used for several applications such as optical filtering in telecommunication, microphones, pressure sensors, and sensing element foe accelerometers.

Silicon MEMS-based optical accelerometers provide higher sensitivity and better reliability, which are key factors in sensor performance, compared to those based on piezoelectric effect or electrical detection [5, 6]. Since these types of sensors use optical power instead of electrical power, they are immune to electromagnetic interference. Optical accelerometers have been investigated previously [5-10], but none of them is fully integrated and moreover most of them are designed for out-of-plane purposes.

The optical accelerometer presented here uses waveguides integrated with MEMS on silicon-on-insulator wafer. It provides an advantageous alternative to conventional accelerometers in terms of size, weight, reliability, and power consumption for future space applications such as navigation systems for microsatellites. Our device is based on in-plane Fabry-Perot filter with DBR mirrors utilizing strip silicon waveguides. Since our FP sensor is in-plane, it allows the integration of all components (DBR mirrors, optical waveguides, proof masses and suspension beams) on a single substrate making it compact and reliable.

CONCEPT

Figure 1 shows the schematic of our proposed optical accelerometer. The deflection of one of the DBR mirrors which is attached to two proof-masses relative to the fixed DBR in the presence of an inertial load causes a shift in the transmitted wavelength. For quasi-static operation, this is given by [9]:

$$a = \frac{-n\omega_n^2 \Delta\lambda}{2} \qquad (1)$$

Where ω_n is the natural frequency of the proof mass structure, $\Delta\lambda$ is the spectral shift, and n is the order of the resonance. It can be seen from this relationship that the sensitivity and resolution of the device is controlled by both optical ($\Delta\lambda$) and mechanical (ω_n) characteristics.

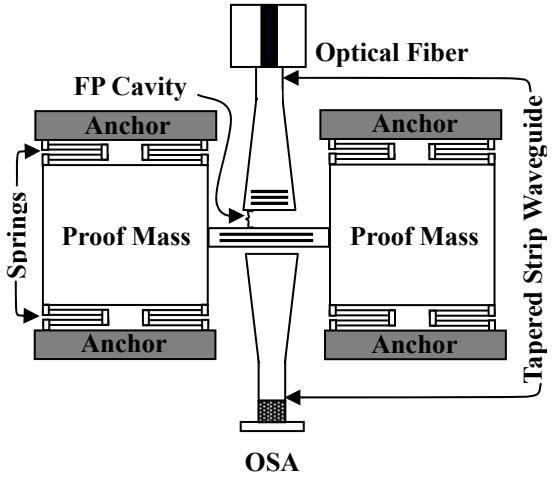

Fig. 1. Schematic of the accelerometer based on FP filter.

Considering an optical spectrum analyzer with a wavelength resolution $\Delta\lambda$ =1pm, the resolution δa is:

$$\delta a = \frac{1(2\pi 405)^2 0.001nm}{2g} = 0.33\,\mu g \qquad (2)$$

for a typical system having a resonant frequency of 405 Hz and resonance order n=1. This demonstrates the potential of a FP based optical accelerometer.

DESIGNS AND FABRICATION

A finite element method is used to model the mechanical behavior of the device. Two proof masses (1.36×10^{-7} kg) are suspended on eight springs (Fig. 1) having a designed overall stiffness of 15 N/m providing 1×10^4 Hz resonant frequency.

A major challenge in the design of accelerometers is to maximize the sensitivity of the device to the desired acceleration axis versus all other cross-axis excitations. Performed micromechanical simulations and design iterations, lead to a cross-axis sensitivity of less than 0.5% for the unwanted in-plane orthogonal axis and 0.01% for the out of plane z-axis. To the best of our knowledge these are the smallest reported cross-axis sensitivities and stiffness for optical accelerometers.

The device fabrication process flowchart is shown in Fig. 2.

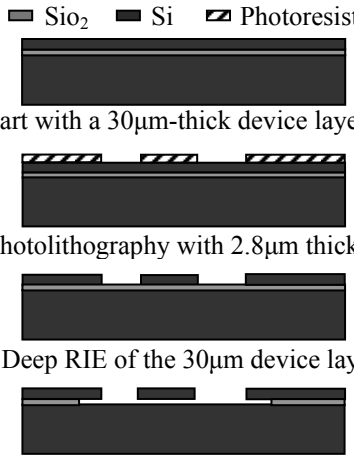

Fig. 2. Microfabrication steps for the FP based accelerometer.

The device is fabricated using one single deep reactive ion etching (DRIE) step on a 30 μm SOI with 3 μm thick buried oxide. 30 μm thick silicon device layer is used in order to have bigger proof mass leading to better sensitivity of the sensor. Suspension beams, proof masses, DBR mirrors, and strip waveguides are fabricated by DRIE. After wafer dicing and polishing, which are critical processes for having waveguides with good quality edges and facets, the remaining buried oxide is removed using vapor HF etching to release the structure and prevent the devices from sticking to the substrate. The fabricated device is shown in Fig. 3. The movable DBR mirror is displaced when exposed to acceleration, producing a reduction in the length of the air gap of the FP filter. The other DBR mirror is positioned at the end of a waveguide collimator. The waveguide collimator is used to reduce the numerical aperture of the beam in the horizontal direction, reducing the divergence of the input beam. A gap of 27.1 μm was considered for the FP cavity to enable its future interrogation using a tunable laser with 30nm dynamic range.

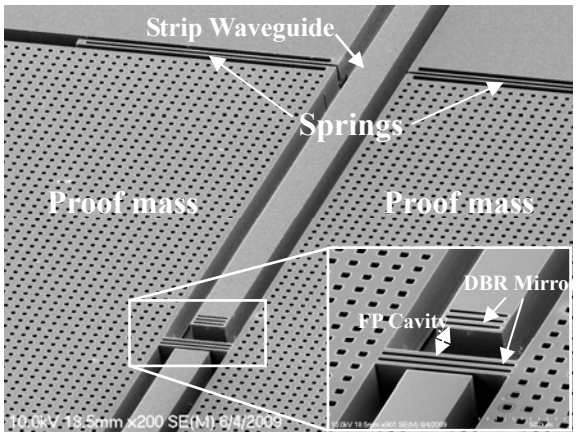

Fig. 3. SEM photograph of the silicon microfabricated FP based accelerometer.

CHARACTERIZATIONS

Experimental setup of the accelerometer is shown in Fig. 4. Light from a broadband source (1520nm-1620nm) is transmitted using butt coupling into the input waveguide through an optical fiber. The transmitted light is collected by the second optical fiber, which is butt coupled to the output tapered waveguide on one side and to an optical spectrum analyzer on the other side. The whole setup is attached to an inclinable board that can be tilted. Acceleration is applied to the device as a consequence of gravity by tilting the board ($g\ sin\theta$). The transmission peak of the FP shifts to shorter wavelength, while increasing the angle of inclination (sensing accelerations from 0 to 0.83g). Figure 5 compares the measured and simulated transmission spectra of the device. The initial transmission peak is 1589.33nm. As acceleration is increased, the air gap between the two Bragg reflectors is decreased resulting in transmission peak shift toward shorter wavelengths. The filter can be tuned continuously down to 1559.33nm for a total tuning range of 30nm. Higher tuning range could be achieved by using a

smaller gap since it would provide a larger free spectral range. The FWHM of the peak is 2.4 nm.

A transfer matrix method is used to simulate the transmitted light across the FP filter by considering a

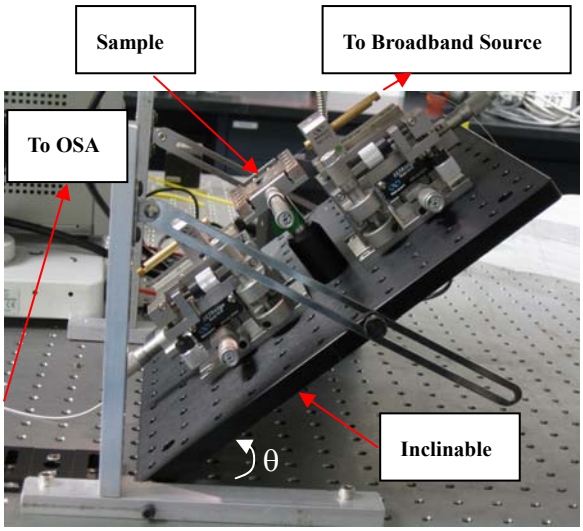

Fig. 4. Optical setup for the characterization of the accelerometer.

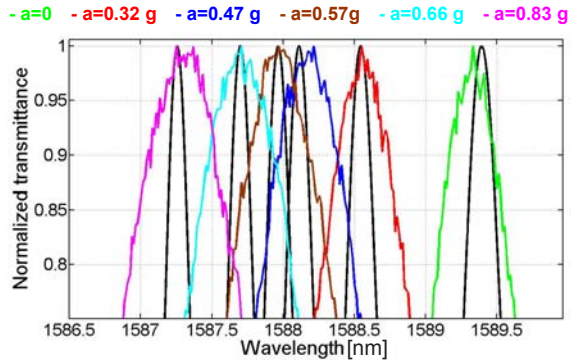

Fig. 5. Measured (colored curves) and simulated (black curves) transmission spectra of the FP based accelerometer.

plane wave incident beam. Because of the deviation of lateral dimensions generated by etching phenomenon in DRIE process, the measured peaks are not exactly at locations predicted by simulations corresponding to resonant frequency of 1×10^4 Hz. Instead, they are all equally deviated by 0.15nm from expected locations. Further investigation shows that these peaks correspond to a resonant frequency of 1.01164×10^4 Hz. This resonant frequency has been considered in the simulation of Fig. 5 to take into account the microfabrication imperfections.

Figure 6 shows the resonant wavelength shift of the FP filter versus applied acceleration. 2.5 nm/g sensitivity is extracted from the curve leading to 400µg resolution for the sensor. The device has a mass of 1.4×10^{-7} kg with a spring constant of 15 N/m resulting to 1670 Hz natural frequency. According to Eq.1 better resolution and sensitivity can be achieved if the natural frequency is lowered and the order of interference is reduced by decreasing the cavity gap.

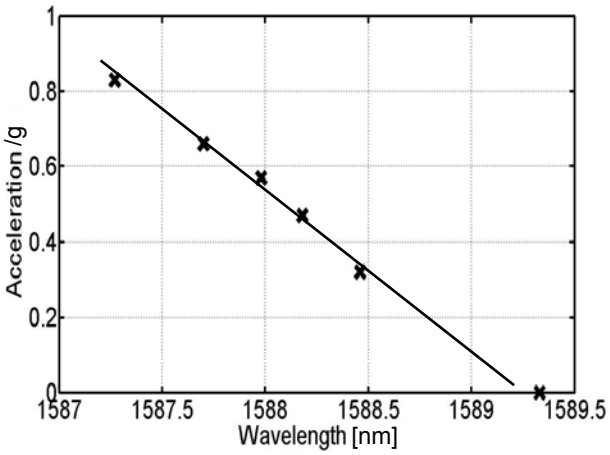

Fig. 6. Measured wavelength shift versus applied acceleration.

CONCLUSION

In conclusion, we have successfully demonstrated a novel design for optical accelerometers with an in-plane sensitive axis. A silicon-on-insulator Fabry-Pérot optical cavity with integrated strip waveguides and deeply etched silicon/air distributed Bragg reflector mirrors was successfully fabricated and fully tested. All optical and mechanical components are integrated on a single substrate making the sensor compact and reliable. The sensor has a theoretical resolution limit below 1µg with a demonstrated 2.5 nm/g sensitivity and 400µg resolution. Experimental results show that the response of the sensor to the applied acceleration is linear. Measured optical characteristics are in good agreement with the predicted ones from numerical simulations. The sensor has a resonance frequency of 10 kHz with a cross-sensitivity lower than 0.5%. 1µg resolution can be achieved (without considering the system noise) if the natural frequency is lowered 10 times and the order of interference is reduced 30 times by designing the sensor with shorter cavity gap. Its simple fabrication process allows fabricating a two-axis accelerometer-structure in a single etching step, by simultaneously putting two sensor elements together rotated by 90° with respect to each other.

ACKNOWLEDGEMENTS

The authors would like to acknowledge the constructive suggestions of Dean Sangiorgi and Linh Ngo-Phong from the Canadian Space Agency.

REFERENCES

[1] W. R. Jamroz, R. Kruzelecky, E. I. Haddad, Applied Microphotonics, CRC press, 2006.

[2] A. Lipson, E. M. Yeatman, "Free-space MEMS tunable optical filter on (110) silicon," IEEE/LEOS Optical MEMS, pp. 73-74, 2005.

[3] S.-S. Yun, K.-W. Jo, J.-H. Lee, "Crystalline Si-based in-plane tunable Fabry-Perot filter with wide tunable range," IEEE/LEOS Optical MEMS, pp. 77-78, 2003.

[4] J. Masson, F. B. Koné and Y.-A. Peter, "MEMS Tunable Silicon Fabry-Perot Cavity," SPIE Optomechatronic Micro/Nano Devices and Components III, Lausanne, Switzerland, October 2007.

[5] W. Noell, P.-A. Clerc, L. Dellmann, B. Guldimann, H.-P. Herzig, O. Manzardo, C. R. Marxer, K. J. Weible, R. Dändliker, and N. de Rooij, "Applications of SOI-based optical MEMS," IEEE J. Select. Topics Quantum Electron., vol. 8, pp. 148–154, 2002.

[6] J. Marty et al., "Fiber-Optic accelerometer using silicon micromachined techniques," Sensors and Actuators A, vol. 46-47, pp. 470-473, 1995.

[7] B. Guldimann, P. Dubois, P.-A. Clerc, N.F. de Rooij, "Fiber Optic– MEMS Accelerometer with high mass displacement resolution," The 11th International Conference on Solid-State Sensors and Actuators, Munich, Germany, June 2001.

[8] S. Baglio1, S. Castorina1, J. Esteve, N. Savalli, "Highly sensitive silicon micro-g accelerometers with optical output, Proceedings of the 2004 International IEEE Symposium on, vol. 4, pp. IV - 868-71, May 2004.

[9] A. Perez and A. M. Shkel, "Design and Demonstration of a Bulk Micromachined Fabry–Perot μg-Resolution Accelerometer," IEEE Sensors Journal, vol. 7, no. 12, pp. 1653-1662, 2007.

[10] E. J. Eklund and A. M. Shkel, "Factors affecting the performance of micromachined sensors based on Fabry-Pérot interferometry," J. Micromech. Microeng., vol. 15, pp. 1770–1776, 2005.